Comparison of Arterial Input Functions by Magnitude and Phase Signal Measurement in Dynamic Contrast Enhancement MRI using a Dynamic Flow Phantom

Sangjune Laurence Lee[1], Warren Foltz[1], Brandon Driscoll[1], Ali Fatemi[1], Cynthia Menard[1], Catherine Coolens[1], and Caroline Chung[1]
[1]*Department of Radiation Oncology, University of Toronto, Toronto, Ontario, Canada*

Introduction: Accurate measurement of the arterial input function (AIF) is critical for meaningful estimation of tumor vascular permeability using various models such as the Toft's model (1). However, slice profile and in-flow effects introduce a spatial dependence to the accuracy of magnitude-derived input functions, while T2* effects typically blunt the input function in a concentration-dependent manner (2). Use of the phase signal could provide an alternative approach for arterial input function quantification, which is robust to each of these factors. The aim of this work is to investigate the accuracy and robustness of magnitude and phase-derived arterial input functions in the controlled environment of an in-house developed dynamic flow phantom at different flow velocities.

Methods: ***Flow Phantom:*** To allow for absolute calibration of flow and comparison of AIF accuracy, an in-house developed flow phantom with modifications for MR compatibility was used [Fig. 1] (3). Physiological flow was generated by a positive displacement pump (Compuflow 1000MR, Shelley Medical Imaging Technologies, London, ON) with contrast being injected through an in-line clinical power injector connected by ¼" PVC tubing. The flow system utilized a 15-85% glycerol-water mixture to mimic blood. 3m of coil tubing was inside the bore to improve the polarization of in-flowing spins. A 50cc centrifuge tube filled with 15% glycerol was placed in the imaging stack to provide a phase reference.

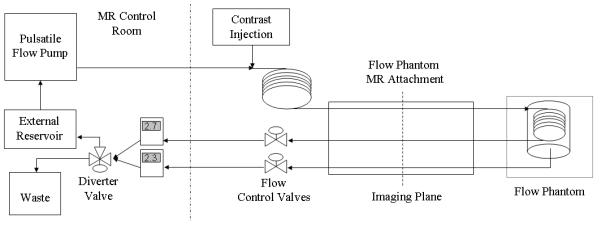

Figure 1: Flow phantom and imaging setup.

MRI: All MRI measurements used a 3T IMRIS Verio system. Both variable-flip-angle (VFA) T_1 measurements and dynamic imaging used a 3D-FLASH technique with matched TE/TR of 1.8/4.8ms, with 1x1x5mm voxels. All acquisitions used the 8-coil spine array, while SNR in dynamic measurements was augmented further by using the 2-coil body array coil in parallel. All VFA-T_1 acquisitions used flip angles of 2, 10, 20, and 30-degrees. Temporal resolution of dynamic scans was 4.2s. ***Experiment 1 – Gd-DTPA T_1 relaxivity in glycerol:*** Serial dilutions of Gd-DTPA from 0-2mM in 15% glycerol and water were imaged in 15cc centrifuge tubes placed above the 8-coil spine array to determine whether glycerol doping affected the T_1 relaxivity of Gd-DTPA. ***Experiment 2 – Characterization of In-flow effects:*** The 3D-FLASH imaging volume was prescribed as a stack of 24 axial sections (5cm thick, 12cm longitudinal volume). VFA-T_1 measurements were performed at 0mL/s flow rate to identify the plateau of the 3D-FLASH slice profile. VFA-T_1 measurements were repeated at flow rates from 0-7.5mL/s to identify the limiting flow rate for significant in-flow within the plateau, and to quantify R_1 relaxation enhancement as a compensation for in-flow in magnitude-derived AIF estimates. ***Experiment 3 – Comparison of phase and magnitude-derived AIF:*** Dynamic experiments were performed at input flow rates of 3, 5, and 7.5mL/s. Gd-DTPA concentration at peak enhancement was programmed at 10mM by varying the dilution of Gd-DTPA within the power injector at constant injection volume of 16mL and duration of 10s (0.029, 0.041, and 0.057mM, respectively). From previous similar CT experiments, we predict peak concentrations to be 9.5, 9 and 8.5mM, respectively, at the imaging plane. The position of injection was 4m upstream of the imaging volume to minimize any transient flow velocity increase at the time of imaging. ***Image Analysis:*** Images were analyzed with MATLAB (MathWorks, Massachusetts, USA). Magnitude and phase signals from dynamic scans were converted to Gd-DTPA concentration using standard validated signal models (4,5). To correct for in-flow, concentration profiles of magnitude-derived AIFs were re-calculated using VFA-T_1 measured under static conditions and at matched flow rates (6). Systematic phase drift were corrected using the static glycerol tube signal.

Results: ***Experiment 1***: The T_1 relaxivity of Gd-DTPA was 9.77mM^{-1}s^{-1} in 15% glycerol and 6.50mM^{-1}s^{-1} in distilled water. ***Experiment 2***: R_1 was approximately linear with flow rate in most slices [Fig. 2a] [7]. A plateau was achieved in the middle 50% of slices with T_1 of 1400ms +/- 50ms with no fluid flow [Fig. 2b]. Outside this plateau region, T_1 estimates were as low as 400ms at the slice profile edge. As volumetric flow was increased from 0 to 7.5mL/s, T_1 progressively dropped to less than 4ms in slices close to the profile edge. ***Experiment 3***: Within the in-flow tube, the peak Gd-DTPA concentrations from magnitude AIF were 300, 400, and 700-fold below the expected peak concentration at flow rates of 3, 5, and 7.5mL/s, respectively. When T_1 measured at matched flows were applied for conversion of signal to Gd-DTPA concentration, estimates improved to 180, 90, and 50-fold reductions [Fig. 3a]. Variation in AIF estimates increased in slices closest to the input flow due to in-flow effects. In comparison, peak Gd-DTPA concentration estimates from the phase AIF peaks were within 29, 8, and 8% of the expected concentration at 3, 5, and 7.5mL/s, respectively [Fig. 3b]. Additionally, the magnitude AIFs showed a susceptibility artifact with a fluctuating signal intensity and misregistration shift in the phase-encoding direction during peak bolus passage [Fig. 4]. In addition the phase AIF estimates were stable between 70 percent of the middle slices with variability dominated by a 25% elevation towards the edges [Fig. 5].

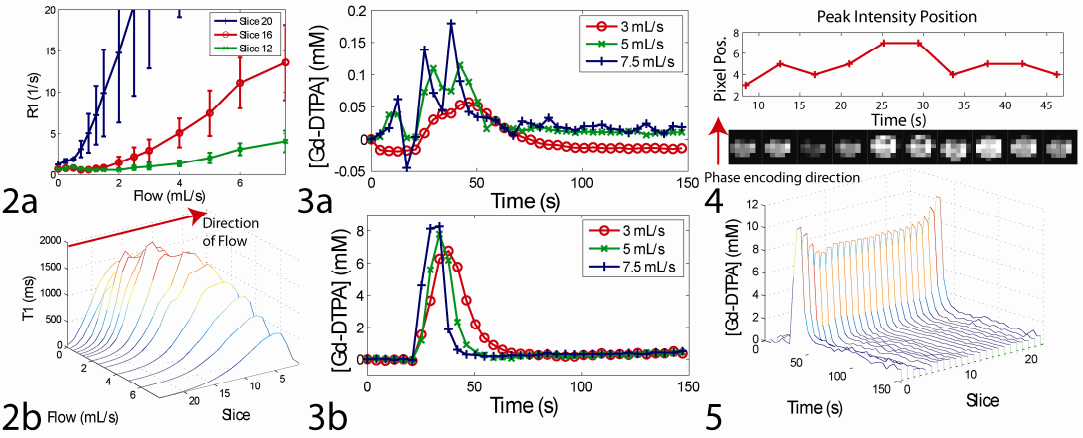

Figure 2: Effect of increasing flow on (**a**) R_1 in slices 20, 16, and 12, and (**b**) T_1 over all slices.
Figure 3: Arterial input function from (**a**) magnitude signal and (**b**) phase signal in slice 12.
Figure 4: Time series cross section of slice 12 showing a susceptibility artifact that shifts the position of the peak intensity pixel in the phase encode direction and causes the signal intensity to fluctuate during peak bolus passage for the 7.5mL/s DCE experiment.
Figure 5: Phase AIF over all slices for the 7.5mL/s DCE experiment.

Conclusions: The phase signal derived AIF is more robust and accurate than the magnitude signal derived AIF. Under the tested conditions, the phase AIF graphs did not suffer from severe in-flow and T_2* effects, compared to the magnitude derived AIFs. In comparison, in-flow compensated magnitude AIF estimates were grossly attenuated, probably because of considerable T_2* signal attenuation, flow-related dephasing, and susceptibility artifacts at peak bolus passage (7). The more reliable phase-derived AIF allows for more confidence and may provide a better approach for AIF acquisition for the clinical investigation of tumor vascular measures. Future work will investigate magnitude AIF performances at lower Gd-DTPA concentrations and further validate phase AIFs by direct comparison to CT derived AIFs.

References: [1] Tofts PS. J Magn Reson Im 1997. [2] Akbudak E. Magn Reson Med 1997. [3] Driscoll B, Med Phys 2011. [4] Cron GO, Magn Reson Med 2005. [5] Landis CS, Magn Reson Med 2000. [6] Bauer WR. Magn Reson Med 1996. [7] Kuribayashi H et al. J Magn Reson Im 2007.